Int. J. Electrochem. Sci., 10 **(2015)** 10104 - 10118

International Journal of
ELECTROCHEMICAL
SCIENCE
www.electrochemsci.org

Corrosion Resistance of UV-Cured Urethane Acrylate Coatings Containing Dibutyl-Substituted Poly(3,4-propylenedioxythiophene) as a Corrosion Inhibitor

Jun Ma[1,2], zhou yufeng[1], Jing Xu[3], Lin Gu[1], Guoqiao Lai[3], Bin Chen[2], Shuan Liu[1,], Haichao Zhao[1,*], Haibin Yu[1], Jianmin Chen[1]*

[1] Key Laboratory of Marine Materials and Related Technologies, Zhejiang Key Laboratory of Marine Materials and Protective Technologies, Ningbo Institute of Materials Technology and Engineering, Chinese Academy of Sciences, Ningbo 315201, P.R. China
[2]School of Materials Science and Engineering Shenyang University of Chemical Technology 11 St. Economic & Technological Development Zone Shenyang 110142, P.R.China.
[3]Key Laboratory of Organosilicon Chemistry and Material Technology of Ministry of Education, Hangzhou Normal University, Hangzhou 310012, P.R.China.
[*]E-mail: liushuan@nimte.ac.cn (S. Liu); zhaohaichao@nimte.ac.cn (H. Zhao)

Received: 26 August 2015 / *Accepted:* 12 October 2015 / *Published:* 4 November 2015

Photopolymerization of urethane acrylate (PUA) containing solution-processable dibutyl-substituted poly(3,4-propylenedioxythiophene) (Poly(ProDotBu$_2$)) was applied on Q235 carbon steel. The corrosion resistance of as-prepared composite coatings with various contents of Poly(ProDotBu$_2$) was studied by electrochemical techniques including open-circuit potential (OCP), potentiodynamic polarization curves and electrochemical impedance spectroscopy (EIS). It was observed that the PUA/Poly(ProDotBu$_2$) composite coatings exhibited an excellent corrosion resistance and barrier properties in comparison with pure PUA coating.

Keywords: Urethane acrylate; Inhibitor; Photopolymerization; EIS; corrosion resistance

1. INTRODUCTION

Corrosion, a electrochemical process when metallic materials are exposed to corrosive environment (O_2, H_2O, Cl^-, HCl, H_2S, etc.), is very costly and has a great impact on the economies of industrialized countries [1]. One of the most convenient strategies for combating corrosion is the use of organic coatings to avoid direct contact between metallic materials and corrosive environments. Conventional organic coatings usually contain hexavalent chromium compounds as a corrosion

inhibitor, which are highly toxic to the environment and human health [2]. Although other environmentally more compliant protective coatings have been developed for provision of cathodic protection as well as barrier protection, they are less effective in some aggressive environments [3-5]. Therefore, it's still a challenge for the development of more environmental friendly coatings for heavy-duty protective coatings.

Since Deberry reported the electrodeposited polyaniline on stainless steel exhibited excellent corrosion resistance in an acidic environment in 1985 [6], intrinsically conducting polymers (ICPs) have been envisaged as one of the most efficient and environment-friendly inhibitors for combating corrosion. In general, two strategies have been proposed for the preparation of ICPs-based anticorrosive coatings. One strategy is the preparation of ICPs-based primer coatings by direct electrodeposition of electroacitve monomers on the metallic surface. Polyaniline, polypyyrole and polythiophene are the most studied conducting polymers for anticorrosion applications because of their ease of synthesis, environmental stability and relative low cost [7-10]. The other strategy is adding miscible ICPS or dispersible ICPs particles into the conventional organic coatings to form composite coatings [11-15]. A little amount of ICPS enables organic coatings to retain their original properties such as mechanical properties and good barrier protection, and also endows organic coating with improved anticorrosive properties due to formation of a passivated layer on metal surface catalyzed by ICPs.

Among all the conducting polymers, 3,4-ethylenedioxythiophene (EDOT) based conducting polymers have been extensively investigated from both scientific and practical fields because of their many advantages including reduced band gap in the polymers, low oxidation potential, and high environmental stability[16-18]. Unsubstituted poly(3,4-ethylenedixythiophene) (PEDOT) is infusible and insoluble, which is difficult to be homogenously incorporated into the polymeric resins. Although the solubility of PEDOT could be enhanced by using a water soluble poly(styrene sulfonate) (PSS) as a doping agent [19, 20], the hydrophilic and charged characteristics of PEDOT/PSS tend to deteriorate the mechanical properties of the coatings [21]. Both Xu group[22] and Liesa group[23] have found that a little amount of PEDOT/PSS in the polymer resin is essential to achieve the coating with enhanced anticorrosive performance. Substituted 3,4-propylenedioxythiophene based conducting polymers show good electro-optical properties similar to those of PEDOT, and exhibit some better properties such as improved processability and solubility[24]. In present study, novel solution-processable dibutyl-sbustituted poly(3,4-propylenedioxythiophene) (Poly(ProDotBu_2)) was synthesized by Grignard metathesis (GRIM) polymerization. UV-cured urethane acrylate coatings (PUA) with various contents of Poly(ProDotBu_2) were applied on Q235 carbon steel substrate. The anticorrosion properties of as-prepared coatings were investigated by open-circuit potential (OCP), potentiodynamic polarization and electrochemical impedance spectroscopy (EIS).

2. MATERIALS AN METHODS

2.1. Materials

All reagents were purchased from Tokyo Chemical Industry (TCI), Sigma-Aldrich, Aladdin, and used without further purification unless otherwise noted. 6,8-dibromo-3,3-dibutyl-3,4-dihydro-2-

H-thieno[3,4-b][1,4] dioxepine ($ProDOTBu_2Br_2$) was synthesized following the literature procedure [25]. UV-curable urethane acrylate (Hexafunctional SARTOMER CN975 NS) was purchased from SARTOMER Company.

2.2 Synthesis of dibutyl-substituted poly(3,4-propylenedioxythiophene) (Poly($ProDotBu_2$).)

A N_2-filled gastight Schlenk tube was charged with $ProDOTBu_2Br_2$, MeMgCl (2 mmol), and anhydrous THF (2.0 mL). The mixture was gradually heated up to 45 °C and kept stirring at this temperature for 50 minutes. Then Ni(dppe)Cl_2 was added and stirred at 323K for one hour in nitrogen atmosphere. The mixtures were then poured into hexane (100 mL), the precipitate was filtered off, and purified by precipitation with a large amount of methanol. The polymer was filtered and dried under vacuum to obtain ferric red solid (51% yield). ^{1}H NMR (400 MHz, $CDCl_3$) δ 3.86 (d, *J* = 92.3 Hz, 4H), 1.41 (dd, *J* = 93.0, 35.2 Hz, 12H), 0.95 (s, 6H).^{13}C NMR (101 MHz, $CDCl_3$) δ 144.97, 113.76, 77.91, 43.77, 31.52, 25.14 (s), 23.57, 14.10.

2.3. Preparation of PUA /Poly($ProDotBu_2$) composite coatings

Q235 carbon steel was used for all the electrochemical studies. The steel specimens were fixed within epoxy resin holder, and the geometric area of the electrode exposed to the electrolyte was 1.0 cm^2. The specimens were carefully abraded with sequence emery papers of various grade (400-800 grit) under a stream of water, degreased with acetone, washed with distilled water, and finally dried in a vacuum. Poly($ProDotBu_2$) (1 wt%, 2.5 wt%, 5 wt%), diphenyl (2,4,6-trimethylbenzoyl)-phosphine oxide (photoinitiator, 0.5 wt%), and urethane acrylate were predissolved in THF and stirred for 1 hour. After the solvent was removed by rotary evaporator, the liquid prepolymer mixtures were applied on the Q235 steel electrode surfaces with a bar coater. The coating thickness was 20±2 μm measured by using a PosiTector6000FNS1 apparatus. The coated electrode was then exposed to UV light (365 nm, 1 kw) for 3 minutes to obtain PAU /Poly($ProDotBu_2$) composite coatings. Pure PUA coatings was also prepared in a similar procedure except the addition of Poly($ProDotBu_2$).

2.4. Measurements

^{1}H NMR and ^{13}H NMR spectra were recorded at room temperature on a NMR spectrometer (400 MHz AVANCE III, Bruker) in $CDCl_3$. The molecular weight (Mn) and molecular weight distribution (Mw/Mn) of the polymers were measured on a Waters GPC system, which was equipped with a Waters 1515 HPLC solvent pump, a Waters 2414 refractive index detector, and two Waters Styragel High Resolution columns, at 313K using HPLC grade THF as eluent at a flow rate of 1.0 mL/min. FTIR spectra were performed on a spectrometer (NICOLET 6700, Thermo) by collecting 32 scans at a spectral resolution of 4 cm^{-1}. UV-vis spectra were obtained using a UV-vis spectrometer (Lambda 950, Perkin-Elmer). Thermo gravimetry analysis (TGA) was tested on a Perkin-Elmer Pyris Diamond thermal analyzer under a N_2 atmosphere at a heating rate of 293 K/min from 303 K to 773 K.

Electrochemical impedance spectroscopy (EIS) was performed on a CHI-660E electrochemical system in 3.5 wt% NaCl aqueous solution. A classical three-electrode cell system was employed, consisting of a coating/Q235 steel as the working electrode, a saturated calomel electrode (SCE) equipped with a Luggin capillary as the reference electrode and a platinum plate of 2.5 cm^2 as the counter electrode. The volume of the cell was 500 ml. All the potentials in this paper were reported in the SCE scale. For EIS, the test frequency range was 10^5-10^{-2} Hz and the amplitude of the sinusoidal voltage signal was 30 mV. EIS data were analyzed by ZsimpWin 3.21 software. Polarization curves were recorded from -200 mV to +200 mV versus open circuit potential (OCP) by changing the electrode potential automatically with a scan rate of 0.5 mV/s. Cyclic voltammetry (CV) measurements were carried out in aqueous HCl solution (1 mol/L), a glass carbon electrode was used as the working electrode, the reference electrode was a saturated calomel electrode equipped with a Luggin capillary, and the counter electrode was a platinum plate. The scan rate was 20 mV/s, all the experiments were carried out at room temperature (about 298K).

To determine the reproducibility of the data, three parallel coating/metal systems were performed for electrochemical test and representative results were selected.

3. RESULTS AND DISCUSSION

3.1. Synthesis and characterization of dibutyl-substituted poly(3,4-propylenedioxythiophene) (Poly(ProDotBu$_2$))

Among all cross coupling reactions used for the synthesis of conjugated polythiophenes, Grignard metathesis (GRIM) is particularly attractive for the synthesis of alkyl-substituted polythiophenes due to its simplicity and cost effectiveness.[26] In present study, GRIM was employed to synthesize dibutyl-substituted poly(3,4-propylenedioxythiophene) (Scheme 1). The polymerization was conducted by preparation of dioxythiophene-magnesium intermediates, and subsequent addition of Ni(dppe)Cl_2 catalyst to initiate polymerization. Poly(ProDotBu$_2$) with moderate molecular weight and narrow molecular weight distribution (M_n=18500, M_w/M_n =1.3) was obtained, which was fully soluble in common organic solvent such as DMF, THF, Chloroform, and ethyl acetate. The ^{1}H and ^{13}C NMR spectra of Poly(ProDotBu$_2$) are well assignable and consistent with the structure of Poly(ProDotBu$_2$) as shown in Fig.1. The electro-optical properties of Poly(ProDotBu$_2$) was investigated by means of UV-Vis-spectroscopy and cyclic voltammetry. Fig. 2A depicts UV-vis spectrum of PolyProDOT(Bu)$_2$. The polymer exhibits the absorption peaks between 540-590 nm, corresponding to the conjugated main chain. The electroactivity of the polymer was studied by CV in the potential range from -0.7 to 0.6 V at a scan rate of 20 mV/s in 1 mol/L HCl solution (Fig. 2B). A board oxidation peak (0.2 V) and reduction peak (-0.1 V) were found at the normal scan rate, and the electrochemical properties are stable since the redox properties are almost unchanged after 100 consecutive oxidation-reduction cycles.

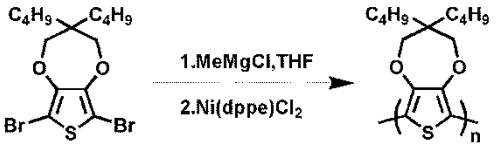

Scheme 1. Schematic illustration of the preparation of Poly(ProDotBu$_2$) by GRIM.

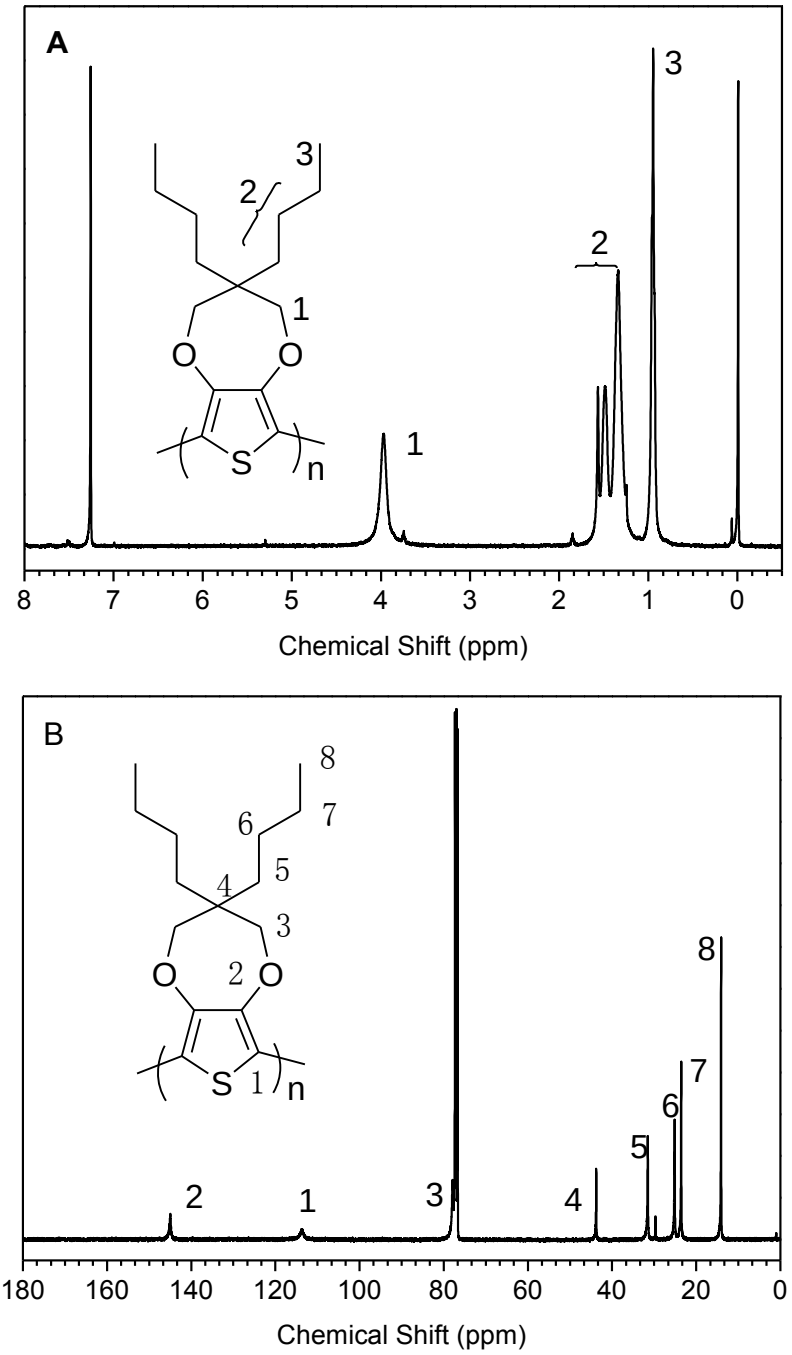

Figure 1. ^{1}H and ^{13}C NMR spectra of Poly(ProDotBu$_2$) measured in $CDCl_3$.

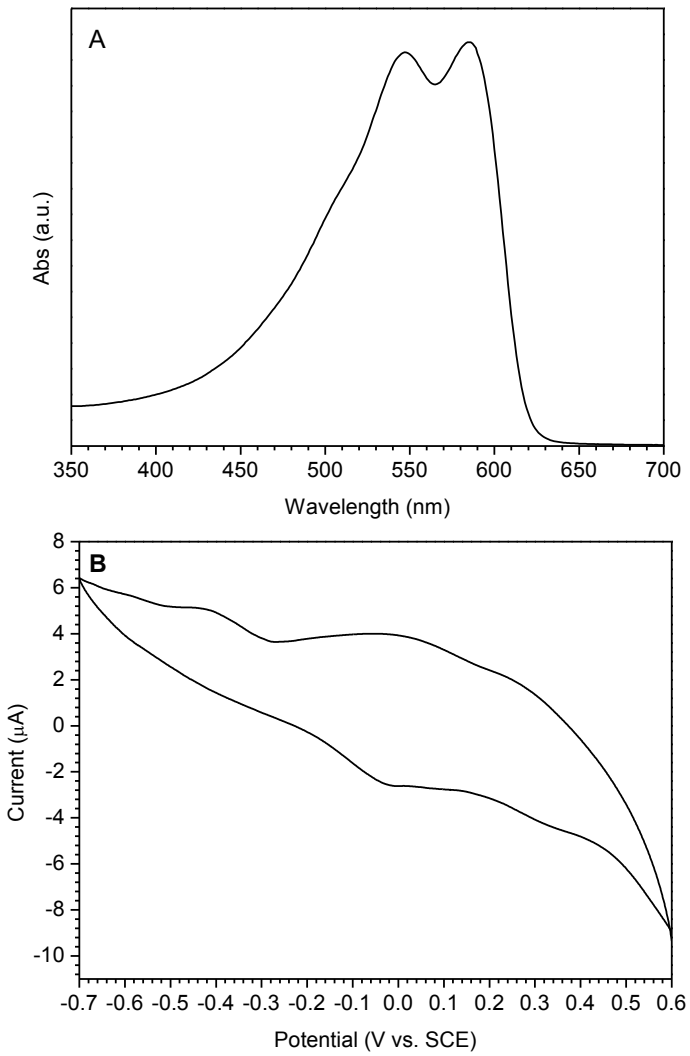

Figure 2. UV-vis spectra (A) of Poly(ProDotBu$_2$) measured in THF at 298K (*c*= 0.01 mol/L) and cyclic voltammograms (B) of Poly(ProDotBu$_2$) deposited on Pt/carbon electrode in 1 mol/L HCl solution at 298K, the counter electrode was a platinum plate and the reference electrode was SCE.

3.2 Preparation and Characterization of PUA /Poly(ProDotBu$_2$) composite coatings

Compared to solvent-borne coatings, UV-curing coating technology provides benefits in terms of low energy costs, reduced environmental impact and a fast curing process. PUA/Poly(ProDotBu$_2$) composite coatings were prepared on Q235 carbon steel using a photopolymerization technique. The composite coatings were characterized by FTIR， TGA and UV-vis spectroscopy. Fig. 3 depicts FTIR spectra of Poly(ProDotBu$_2$), urethane acrylate, pure PUA, and PUA/Poly(ProDotBu$_2$) composite coatings, respectively. As shown in Fig. 3A, the absorption bands of Poly(ProDotBu$_2$) at 2963, 1478, 1039, 1426, and 1375 cm^{-1} are associated with C-H stretching, C=C stretching of thiophene ring, C-O stretching of dioxythiophene ring, C-H bending of CH_2 and CH_3, respectively. The typical absorption bands of urethane acrylate monomer at 3351, 1731, 1635 and 810 cm^{-1} are assigned to –NH stretching,

C=O stretching, C=C vibration and CH alkene twisting, respectively (Fig 3B). The significant weakness of the absorption peaks at 1635 and 810 cm^{-1} for PUA and PUA/Poly(ProDotBu$_2$) composites coatings and the formation of thin film on the steel indicate successful photopolymerization (Fig. 3Cand Fig.3D).

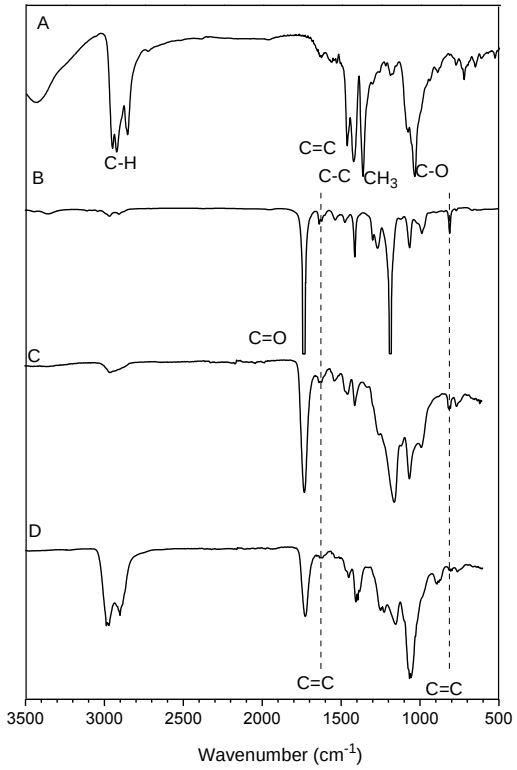

Figure 3. FITR spectra of (A) Poly(ProDotBu$_2$), (B) urethane acrylate; (C) UV-cured PUA (D) PUA with 2.5 wt % Poly(ProDotBu$_2$).

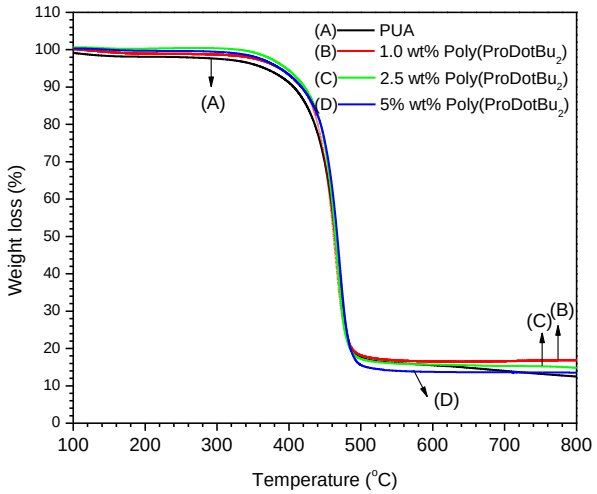

Figure 4. TGA curves of PUA coating and PUA coatings containing different contents of Poly(ProDotBu$_2$).

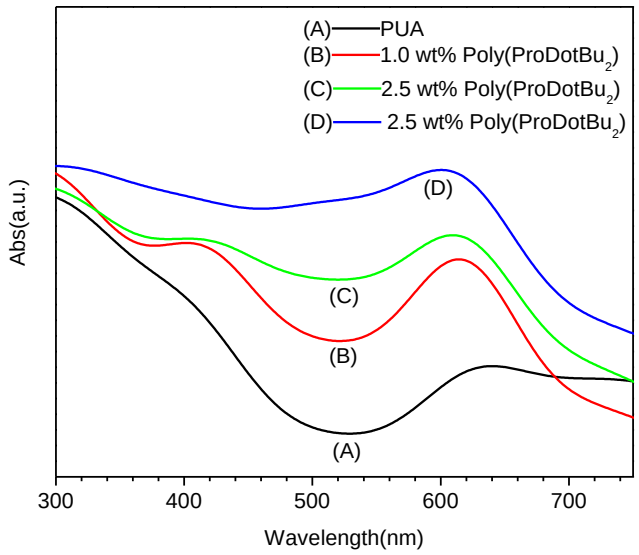

Figure 5. UV-vis spectra of PUA film and PUA films containing different contents of Poly(ProDotBu$_2$).

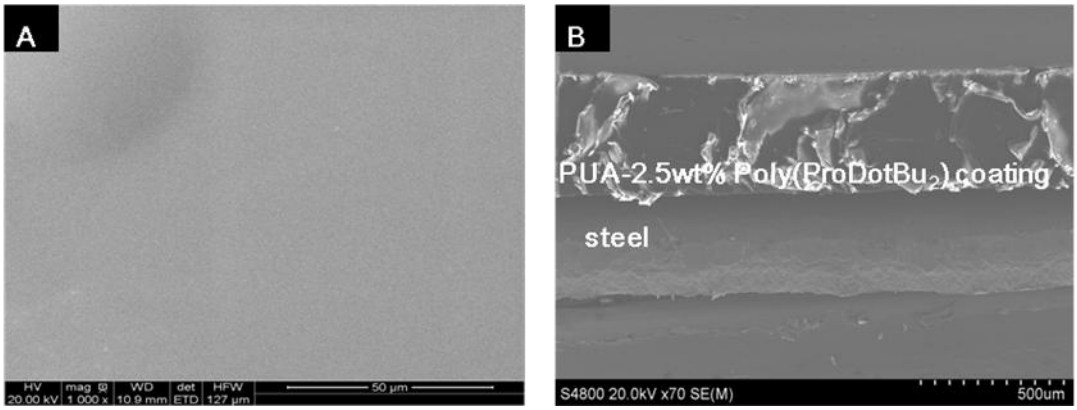

Figure 6. SEM images of (A) surface morphology of PUA-2.5wt% Poly(ProDotBu$_2$) and (B) cross-section of PUA-2.5wt% Poly(ProDotBu$_2$)/steel interface.

The thermal stability of the fabricated coatings was investigated by TGA (Fig. 4). All the coatings are thermally stable up to 300 ^{o}C. The coatings underwent thermal degradation from 300 $^{\circ}$C and with a total 80% mass loss at 500 ^{o}C. All the as-prepared coatings are transparent and exhibit board UV-vis absorption at around 620 nm (Fig. 5), indicating that Poly(ProDotBu$_2$) was well dispersed in PUA film coatings. The representative SEM images of PUA/Poly(ProDotBu$_2$) composite coatings surface and cross section of PUA composite coating/steel interface are shown in Fig. 6. The coupling between the composite coating and the substrate metal are strongly formed, and no obvious micro-pores or micro-cracks are observed on coating surface, which are beneficial to the protection of Q235 steel against corrosion.

3.3 Open circuit potential measurements

The variations of OCP for PUA coatings with different contents of Poly(ProDotBu$_2$) were recorded against time in 3.5% NaCl solution at 25 ^{o}C. Fig. 7 shows the time dependence of OCP for PUA coatings without and with 1 wt%, 2.5 wt%, 5 wt% Poly(ProDotBu$_2$) load, respectively. The OCP of pure PUA exhibits a slightly negative shift (from -0.60 V of 12-hour immersion to -0.62 V of 96-hour immersion), probably due to the occurrence of some surface phenomenon such as the diffusion of water molecule or chloride ions to the steel surface [27]. All the OCP of the PUA/Poly(ProDotBu$_2$) coatings gradually shifted to the more noble values with immersion time. The OCP values of the composite coatings were found to be -0.53 V (1 wt% Poly(ProDotBu$_2$)) , -0.32 V (2.5 wt% Poly(ProDotBu$_2$)) and -0.51 V (5 wt% Poly(ProDotBu$_2$)) after 96-hour immersion, which are more positive than that of pure PUA coating (-0.60 V). The positive potential shift indicated that the existence of Poly(ProDotBu$_2$) favored the oxidation of the ferrous ions to the stable passive iron oxide film, thus protecting metallic substrate against corrosion. Particularly, the PUA coating with 2.5 wt% poly(ProDotBu$_2$) is 0.31 V more positive than that of pure PUA coating, demonstrating its good corrosion resistance. The OCP of composite coating with 5 wt% of Poly(ProDotBu$_2$) is much lower to that of coating with 2.5 wt% Poly(ProDotBu$_2$), probably due to the deterioration of coating film with the existence of larger amount of Poly(ProDotBu$_2$).

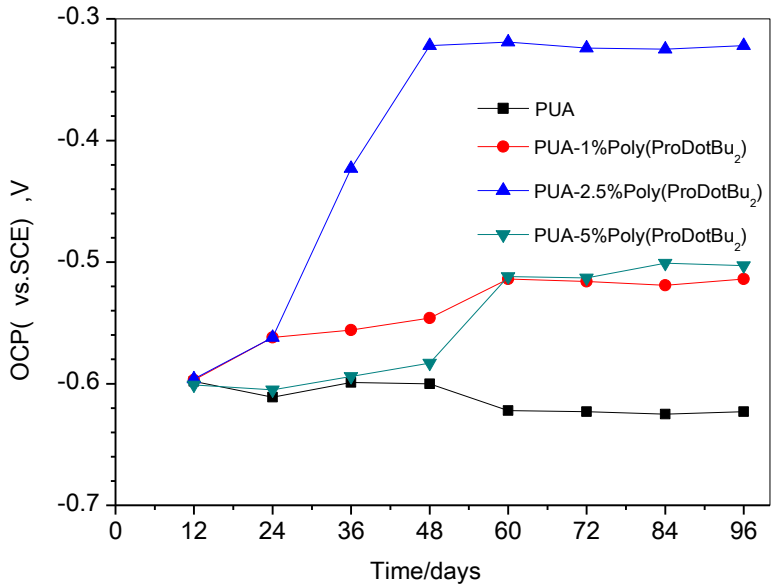

Figure 7. Time dependence of OCP of PUA coating and PUA coatings containing different contents of Poly(ProDotBu$_2$) immersed in 3.5% NaCl solution at 298K.

3.4 Potentiodynamic polarization studies of PUA/Poly(ProDotBu$_2$) composite coatings

Potentiodynamic polarization curves of PUA/Poly(ProDotBu$_2$) coatings after 96-hour immersion are shown in Fig. 8. The values of corrosion current density i_{corr}, corrosion potential E_{corr}, anodic and cathodic Tafel slopes (b_a and b_c) determined from Tafel zone (±30mV with respect to the

E_{corr}), polarization resistance R_p for the composite coatings in 3.5% NaCl solution were listed in Table 1. All the corrosion parameters are determined simultaneously by CorrView software.

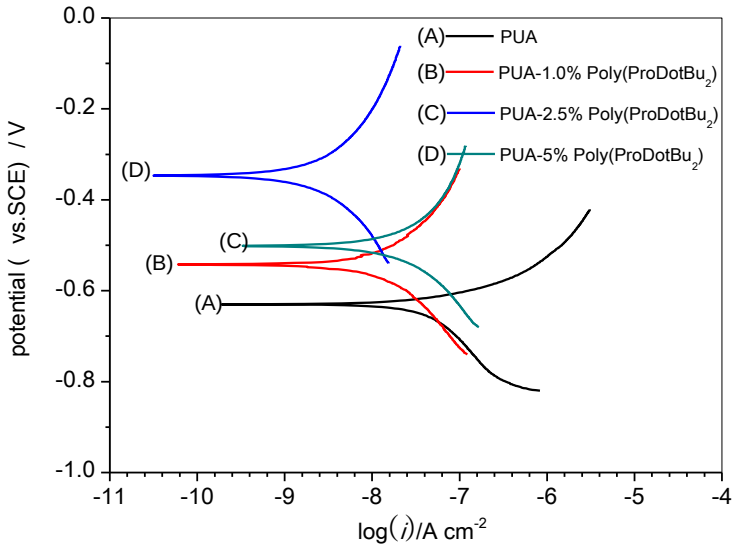

Figure 8. Polarization curves of PUA coating and PUA coatings containing different contents of Poly(ProDotBu$_2$) immersed in 3.5% NaCl solution at 298K after 96 hours.

Table 1. Corrosion parameters for corrosion of PUA coating and PUA coatings containing different contents of Poly(ProDotBu$_2$) immersed 3.5% NaCl solution after 96 hours.

	E_{corr} V, vs.SCE	i_{corr} μA cm^{-2}	b_a mV dec^{-1}	b_c mV dec^{-1}	R_p kΩ cm^2
PUA	-0.621	0.0892	116.9	-178.2	226.4
PUA-1.0%Poly(ProDotBu$_2$)	-0.544	0.00768	240.1	-223.8	2591
PUA-2.5%Poly(ProDotBu$_2$)	-0.362	0.00131	316.4	-208.3	15190
PUA-5.0%Poly(ProDotBu$_2$)	-0.514	0.0231	273.4	-181.8	865.8

For PUA coating, the E_{corr} and i_{corr} are calculated from the Tafel region are -0.62 V and 8.92×10^{-8} A cm^{-2}, respectively. With the addition of Poly(ProDotBu$_2$), the polarization curves show a significant upward shift (more positive corrosion potential) and left shift (lower corrosion current density). The i_{corr} of the composite coatings with 1.0 wt%, 2.5 wt% and 5.0 wt% Poly(ProDotBu$_2$) are 7.68×10^{-9}, 1.31×10^{-9} and 2.31×10^{-8} A cm^{-2}, respectively. Besides, the R_p Values of composite coatings are higher than that of thePUA coating. The changes of Tafel slopes (b_a and b_c) with the increase of Poly(ProDotBu$_2$) suggest that the as-prepared composite coating inhibit both the cathodic and anodic reaction, and Poly(ProDotBu$_2$) acts as a good inhibitor in PUA coating. Especially, the coating with

2.5 wt% Poly(ProDotBu$_2$) exhibits the highest E_{corr} and the lowest i_{corr}, indicating the best corrosion resistance. This positive result is attributed to the high electrochemical activity displayed by Poly(ProDotBu$_2$) and this similar phenomenon was also observed in epoxy paints with small amount of poly(3,4-ethylenedioxythiophene)/poly(styrene sulfonate)[22]. Poly(ProDotBu$_2$) acts as an intermediate and catalyzed oxidization of metal to form a passivated layer on steel surface, which resists the attack of oxygen, H_2O and corrosive ions toward metal.

3.5 Electrochemical Impedance Spectroscopic studies of PUA/Poly(ProDotBu$_2$) coatings

EIS technique was employed to further determine the corrosion behavior of composites coatings. Fig. 9 shows typical Nyquist and Bode diagrams of PUA and PUA/Poly(ProDotBu$_2$) coatings. Bode plot provides information about coating impedance behavior, which is related to the corrosive resistance of the coatings. All the coatings show two capacitive loops because of water or oxygen penetration into the coatings during the immersion, thus, we choose the equivalent circuit model R(Q(R(QR))) (see Fig.10) to fit the EIS data [28]. Generally, the higher impedance modulus at low frequencies indicates the lower defects of the coatings and the better corrosion resistance. The impedance modulus of PUA coating at low frequency ($|Z|_{0.01Hz}$) is 1.04×10^6 Ω cm^2 after the 12-hour immersion, and the resistance values of composite coatings are 5.75×10^7 (1.0 wt% Poly(ProDotBu$_2$)), 1.78×10^8 (2.5 wt% Poly(ProDotBu$_2$)), and 3.99×10^7Ω cm^2 (5.0 wt% Poly(ProDotBu$_2$)), respectively. The impedance modulus of neat PUA coating decreased significantly with the increase of immersion time. It was reduced to only one fifth of initial modulus after 96-hour immersion, indicating the failure of coating. Obviously, the impedance modulus recorded for the composite coatings are much higher than that of the PUA coating, implying their better protective performance [29].

A quantitative investigation of corrosion behavior of composite coatings were conducted by fitting EIS data with equivalent circuit (Fig. 10), and the fitted corrosion electrochemical parameters were listed in Table 2. In the equivalent circuit, R_s is the solution resistance, R_c and Q_c are coating resistance and coating capacitance, respectively. R_{ct} and Q_{dl} are the charge-transfer resistance and double-layer capacitance, respectively [30, 31]. Generally, R_c and R_{ct} of the coatings decreased with immersion time due to the penetration of corrosive media, Q_c and Q_{dl} of the coatings increased due to water uptake [32, 33]. As shown in Table 2, both of the R_c and R_{ct} of PUA coating decreased rapidly with immersion time, while the R_c and R_{ct} of PUA/Poly(ProDotBu$_2$) were much higher than those of pure PUA coating. For neat PUA coating, the R_c values of neat PUA coating decreased from 3.81×10^5 Ω cm^2 to 5.12×10^3 Ω cm^2, and the R_{ct} values of neat PUA coating decreased from 1.46×10^5 Ω cm^2 to 2.53×10^5 Ω cm^2 after 96 hours. When different contents of Poly(ProDotBu$_2$) were added into the PUA, the EIS spectra of PUA-1.0% Poly(ProDotBu$_2$), PUA-2.5% Poly(ProDotBu$_2$) and PUA-5.0% Poly(ProDotBu$_2$) coatings were different from that of the PUA coating and the decrease of impedance values were minor.

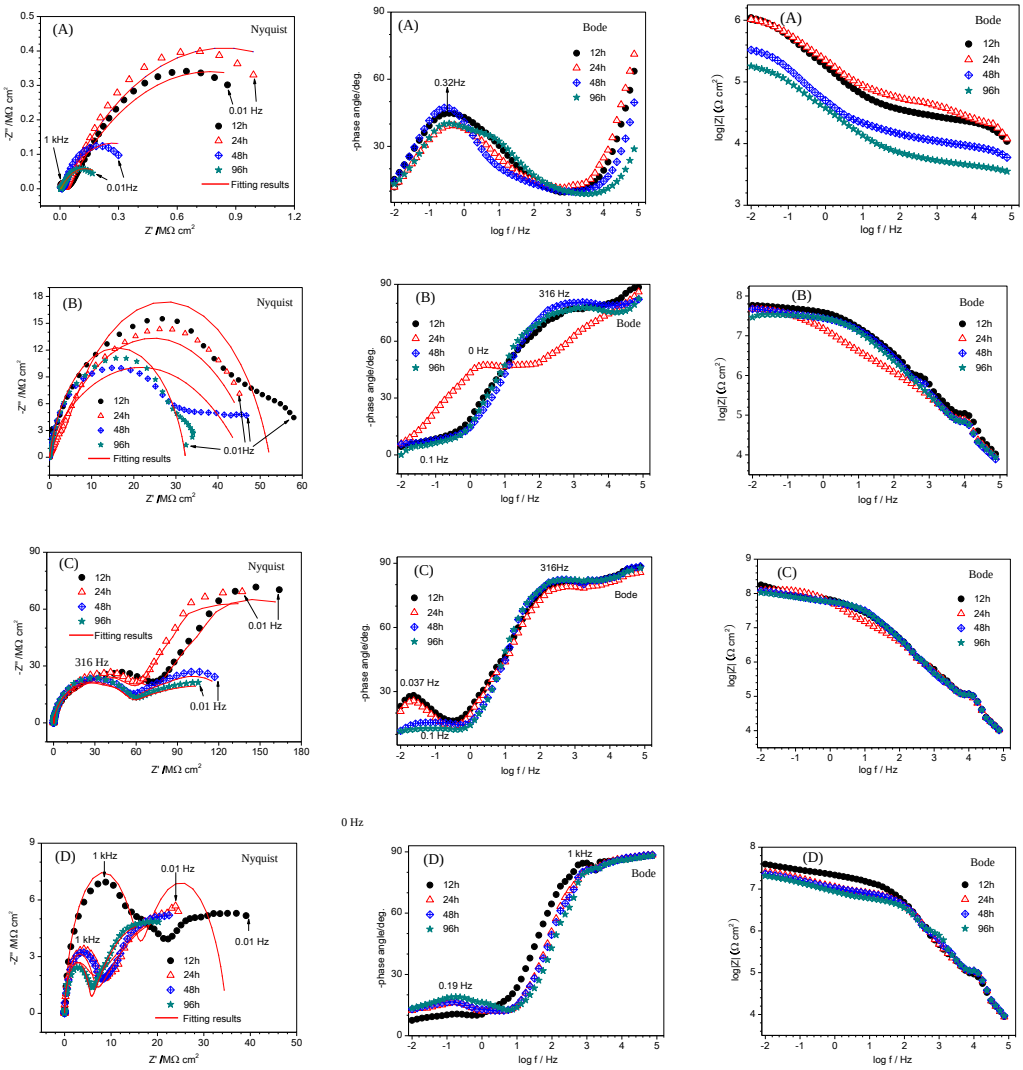

Figure 9. EIS spectrum obtained after different immersion times 3.5%NaCl solution at 298K by (A) PUA coating; (B) PUA with 1 wt% Poly(ProDotBu$_2$); (C) PUA with 2.5 wt% Poly(ProDotBu$_2$) and (D) PUA with 5 wt% Poly(ProDotBu$_2$), respectively. The solid red lines in the Nyquist plots are fitted results.

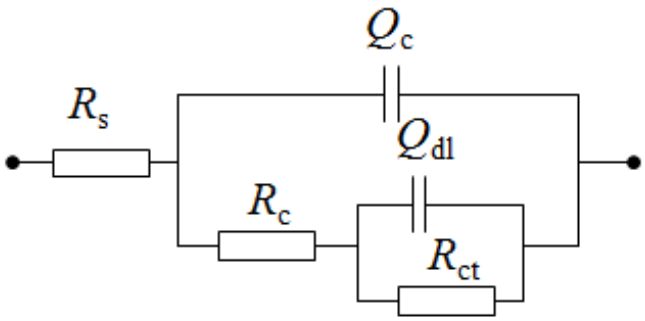

Figure 10. Equivalent circuit used to fit the EIS of PUA coating and PUA coatings containing different contents of Poly(ProDotBu$_2$).

Table 2. The electrochemical corrosion parameters of PUA coating and PUA coatings containing different contents of Poly(ProDotBu$_2$) immersed 3.5% NaCl solution after different immersion times

content	Time hours	R_s Ω cm^2	Q_c nF cm^{-2}	n_1	R_c MΩ cm^2	Q_{dl} μF cm^{-2}	n_2	R_{ct} MΩ cm^2
PUA	12	0.001	0.178	0.91	0.038	169	0.56	1.46
	24	0.001	0.868	0.87	0.026	194	0.59	1.63
	48	0.001	1.73	0.68	0.012	7.71	0.59	0.52
	96	0.001	2.32	0.67	0.005	9.59	0.56	0.25
PUA-1.0% Poly(ProDotBu$_2$)	12	0.001	3.48	0.81	0.912	0.0153	0.72	46.4
	24	0.001	5.31	0.83	0.787	0.0371	0.89	38.9
	48	0.001	58.7	0.85	0.321	0.011	0.51	25.1
	96	0.001	99.1	0.81	0.111	0.526	0.41	24.7
PUA-2.5% Poly(ProDotBu$_2$)	12	0.001	0.128	0.83	35.2	0.0521	0.59	108
	24	0.001	0.537	0.85	28.1	0.0837	0.61	93.1
	48	0.001	0.845	0.83	27.6	0.127	0.74	52.1
	96	0.001	1.21	0.81	27.4	0.226	0.73	51.9
PUA-5.0% Poly(ProDotBu$_2$)	12	0.001	0.349	0.93	15.7	0.0329	0.78	19.2
	24	0.001	0.617	0.91	9.82	0.198	0.56	16.7
	48	0.001	0.737	0.71	8.73	0.574	0.91	7.97
	96	0.001	9.38	0.78	6.33	0.859	0.52	6.85

For the EIS spectra of PUA containing 1% or 2.5% Poly(ProDotBu$_2$) (Fig.9B and Fig.9C), their R_c values initially decreased to some extent with time and then reached a constant value after 24 hours. The impedance modulus recorded for these two coatings were obviously higher than that of the APU coating, indicating the good barrier properties and high ohmic resistance of Poly(ProDotBu$_2$). Especially, after the immersion of 96-hour, the R_c and R_{ct} values of PUA-2.5% Poly(ProDotBu$_2$) coating were 2.74×10^7 Ω cm^2 and 5.19×10^7 Ω cm^2, respectively. The Q_c and Q_{dl} values of PUA-2.5% Poly(ProDotBu$_2$) coating were increased from 0.128 to 1.21nF cm^{-2}, and from 52.1 to 226 nF cm^{-2}, respectively, which were lower than that of other three coating, implying the best barrier property and corrosion resistance of PUA-2.5% Poly(ProDotBu$_2$) coating [34, 35].

However, the corrosion resistance of the PUA-5.0% Poly(ProDotBu$_2$) coating decreased to some extent compared with other coatings. Both of R_c and R_{ct} the values were lower than that of PUA-2.5% Poly(ProDotBu$_2$) coating and PUA-1.0% Poly(ProDotBu$_2$) coating, and its Q_c and Q_{dl} values were higher than PUA-2.5% Poly(ProDotBu$_2$) coating, indicating that the film-forming property was affected and may be destroyed to some extent by the a large amount of Poly(ProDotBu$_2$).

4. CONCLUSION

In summary, we have successfully prepared UV-cured urethane acrylate coatings containing solution-processable dibutyl-substituted poly(3,4-propylenedioxythiophene) (Poly(ProDotBu2). OCP measurements of the composite coatings clearly revealed that the passivation characteristics of coatings with the existence of Poly($ProDotBu_2$). EIS results further confirmed that the coating with 2.5 wt% Poly($ProDotBu_2$) exhibited the best anticorrosive performance. The electroactive Poly($ProDotBu_2$) catalyzed ferrous ions to form a passivated layer on steel surface, and thus resisted the attack of oxygen, H_2O and corrosive ions toward metal. The present research shows that Poly($ProDotBu_2$) is a promising corrosion inhibitor for heavy metal-free organic coatings.

ACKNOWLEDGEMENTS
This research is supported by the financial support of the Ningbo Natural Science Foundation (2015A610016), National Science Foundation of China (No. 41506098, 21404112) and Open Foundation Grant LMMT-KFKT-2014-008 from Key Laboratory of Marine Materials and Related Technologies.

References

1. A. Krishnamurthy, V. Gadhamshetty, R. Mukherjee, Z. Chen, W. Ren, H.M. Cheng, *Carbon.* 56(2013) 45.
2. S.D. Zhang, W.L. Zhang, S.G. Wang, X.J. Gu, J.Q. Wang, *Corros. Sci.*, 93 (2015) 211.
3. H. Vakili, B. Ramezanzadeh, R. Amini,*Corros. Sci*. ,94 (2015) 466.
4. A. Gergely, I. Bertoti, T. Toeroek, E. Pfeifer, E. Kalman, *Prog. Org. Coa*t., 76(2013)17.
5. M.C Yan , C. Sun, J. Xu, T.Q Wu, S. Yang, W.Ke, *Corros. Sci*., 93 (2015) 27
6. D.W. DeBerry, *J. Electrochem. Soc.*, 132 (1985)1022.
7. E. Armelin, C. Aleman, J.I. Iribarren, *Prog. Org. Coat.*, 65(2009) 88.
8. D. V. Huerta, S.R. de Moraes, A.D. Motheo, *J. Solid State Electrochem.*, 9(2005)416.
9. J.L. Camalet, J.C. Lacroix, S. Aeiyach, K.I.C. Ching, P.C. Lacaze, *Synth. Met*., 102(1999)1386.
10. M.N. Shabani, S.M. Ghoreishi, Y. Jafari, N. Kashanizadeh, *J. Polym. Res.*, 21(2014) 415.
11. W. Sun, L.D. Wang, T.T. Wu, Y.Q. Pan, G.C. Liu, *Carbon*., 79(2014) 605.
12. A. Olad, M. Barati, H. Shirmohammadi, *Prog. Org. Coat.*, 72(2011)599.
13. A. Olad, M. Barati, S. Behboudi, *Prog. Org. Coat*., 74(2012)221.
14. F. Chen, P. Liu. *ACS Appl. Mat. Interfaces*., 3(2011)2694.
15. R.C. Rathod, V.K. Didolkar, S.S. Umare, B.H. Shambharkar, *Trans. India Inst. Met.*, 64(2011) 431.
16. Z. Ren, D. Yang, J. Liu, Y. Wang, S. Zheng, *Mater. Prot.*, 47(2014)15.
17. T. Bashir, F. Bakare, B. Baghaei, A.K. Mehrjerdi, M. Skrifvars, *Iran. Polym. J.*, 22(2013)599.
18. M. Balog, H. Rayah, D. Le, M. Sallé, *New J. Chem*. 32(2008)1183.
19. M. Lefebvre, Z.G. Qi, D. Rana, *P.G. Pickup. Chem. Mater.*, 11(1999)262.
20. C.A. Dai, C.J. Chang, H.Y. Chi, H.T. Chien, W.F. Su, W.Y. Chiu, *J. Polym. Sci*., Part A: Polym. Chem. 46(2008)2536.
21. H.B. Bu, G. Götz, E. Reinold, A. Vogt, R. Azumi, J.L.Segura, *Chem. Commun*. 48(2012)2677.
22. J. Hou, G. Zhu, J. Xu, H. Liu, *J. Mater. Sci. Technol*., 29(2013)678.
23. F. Liesa, C. Ocampo, C. Aleman, E. Armelin, R. Oliver, F. Estrany, *J. Appl. Polym. Sci*., 102(2006)1592.
24. E.M. Galand, J.K. Mwaura, A.A. Argun, K.A. Abboud, T.D. McCarley, J.R. Reynolds, *Macromol.*,

39(2006)7286
25. D.M. Welsh, L.J. Kloeppner, L. Madrigal, M.R. Pinto, B.C. Thompson, K.S. Schanze, *Macromol.*, 35(2002)6517.
26. M.C. Iovu, C.R. Craley, M. Jeffries-El, A.B. Krankowski, R. Zhang, T. Kowalewski, *Macromol.*, 40,(2007)4733.
27. G. Ruhi, H. Bhandari, S.K. Dhawan, *Prog. Org. Coat.*, 77(2014)1484.
28. Y S Hao , F C Liu, E H Han, SAnjum, G B Xu, *Corros. Sci*., 69 (2013) 77.
29. M. Behzadnasab, S.M. Mirabedini, K. Kabiri, S. Jamali, *Corros. Sci.*, 53(2011)89-98.
30. Q.L.Cheng and Z. Y. Chen, *Int. J. Electrochem. Sci.*, 8(2013)282.
31. E. M. Sherif and A. A. Almajid, *Int. J. Electrochem. Sci*., 10(2015)34.
32. S. Liu, H. Sun, L. Sun, H.J. Fan, *Corros. Sci.*, 65(2012)520.
33. H.Y. Sun, S. Liu, L.J. Sun, *Int. J. Electrochem. Sci*. 8(2013)3494.
34. L. Gu, S. Liu, H.C. Zhao and H. B. Yu, *RSC Adv*., 5(2015)56011.
35. L. Gu, S. Liu, H.C. Zhao and H. B. Yu, *ACS Appl. Mater. Interfaces*., 7(2015)17641.